

Plasmin Cleavage of the Amyloid β -Protein: Alteration of Secondary Structure and Stimulation of Tissue Plasminogen Activator Activity[†]

William E. Van Nostrand* and Margaret Porter

Departments of Medicine and Pathology, Health Sciences Center, State University of New York, Stony Brook, New York 11794-8153

Received March 17, 1999; Revised Manuscript Received May 24, 1999

ABSTRACT: Cerebrovascular amyloid β -protein ($A\beta$) deposition, a key pathological feature of Alzheimer's disease and hereditary cerebral hemorrhage with amyloidosis Dutch-type, can lead to intracerebral hemorrhage; however, the mechanism for this remains unclear. Assembled $A\beta$ is a potent stimulator of tissue-type plasminogen activator (tPA) in vitro. Herein, we investigated the stimulation of tPA by freshly solubilized $A\beta_{1-40}$. The rate of tPA stimulation by $A\beta_{1-40}$ increased dramatically over time, suggesting that $A\beta$ may be altered during the course of the reaction. SDS-PAGE analysis showed that $A\beta_{1-40}$ was cleaved during the course of the reaction. Subsequent studies showed that it was plasmin, the product of tPA activation of plasminogen, that specifically cleaved $A\beta_{1-40}$ in the amino terminal region between Arg⁵ and His⁶. Plasmin effectively cleaved a chromogenic substrate corresponding to this cleavage site in $A\beta$. Circular dichroism spectral analysis showed that $A\beta_{6-40}$ adopted a strong β -sheet secondary structure. This truncated $A\beta_{6-40}$ peptide was a potent stimulator of tPA in vitro. Our results indicate that β -sheet secondary structure of $A\beta$, which can be promoted by plasmin cleavage, stimulates tPA activity. These findings suggest that pathologic interactions between $A\beta$, tPA, and plasmin in the cerebral vessel wall could result in excessive proteolysis contributing to intracerebral hemorrhages.

Cerebral amyloid angiopathy (CAA)¹ is an age-associated condition that is pathologically characterized by deposition of amyloid in the medial layer of primarily small and medium-sized arteries and arterioles of the cerebral cortex and leptomeninges (1–3). This condition accounts for up to 20% of the cases of primary intracerebral hemorrhage and is a key pathologic lesion in patients with Alzheimer's disease (AD) and hereditary cerebral hemorrhage with amyloidosis Dutch-type (HCHWA-D) (4–7). In contrast to AD, the cerebrovascular amyloid deposition in HCHWA-D occurs earlier in life and is so severe that it leads to recurrent, and often fatal, intracerebral hemorrhages by a mean age of fifty years (6–8). The CAA observed in patients with AD, and patients with HCHWA-D, share a common amyloid subunit known as the amyloid β -protein ($A\beta$) (6, 9, 10). In addition to the walls of the cerebral blood vessels, $A\beta$ is also found deposited in plaques within the neuropil of patients with either of these disorders (for recent review see 11, 12). $A\beta$ is 39–42 amino acid peptide that has the propensity to self-assemble into insoluble, β -pleated sheet-containing fibrils (13). The $A\beta$ peptide is proteolytically

derived from a set of large transmembrane precursor proteins, termed the amyloid β -protein precursors ($A\beta$ PP) (11, 12). The reason that cerebrovascular $A\beta$ deposition leads to loss of vessel wall integrity and hemorrhagic stroke in patients with CAA remains unclear. However, inhibition of the coagulation process, stimulation of plasminogen activation, and degeneration of smooth muscle cells within the vessel wall have all been postulated to play a role (8, 14–17).

Plasminogen activators are serine proteinases that catalyze the conversion of the inactive zymogen plasminogen into plasmin, another serine proteinase. Studies by Kingston et al. (15) showed that assembled forms of $A\beta$ can stimulate the enzymatic activity of tissue-type plasminogen activator (tPA) in vitro. These studies stemmed from the earlier findings that anti- $A\beta$ antibodies crossreact with conformational epitopes on human fibrinogen and that anti-fibrinogen antibodies crossreact with $A\beta$, suggesting structural similarities (18). The in vitro findings of fibrin-mimicry by $A\beta$ could help explain why patients with CAA that are administered therapeutic tPA for acute myocardial infarction suffer from a high incidence of intracerebral hemorrhage (19, 20). The subsequent activation of plasminogen could result in excessive proteolysis leading to loss of vessel integrity and rupture. Furthermore, HCHWA-D patients, with their exaggerated cerebrovascular $A\beta$ deposition, would be even more inclined to suffer from excessive plasminogen activation.

Herein, we show that the product of tPA mediated plasminogen activation, plasmin, specifically proteolyzes $A\beta$ in a manner such that it enhances the β -sheet secondary properties of the peptide. This in turn leads to enhanced stimulation of tPA activity and more robust plasminogen

[†] This work was supported by National Institutes of Health Grants HL49566 and Research Career Development Award HL03229.

* Address correspondence to: Dr. W. E. Van Nostrand, Department of Medicine, HSCT-15/081, State University of New York, Stony Brook, New York 11794-8153. Telephone: (516) 444-1661. Fax: (516) 444-7518. E-mail: wevn@mail.som.sunysb.edu.

¹ The abbreviations used are: CAA, cerebral amyloid angiopathy; $A\beta$, amyloid β -protein; AD, Alzheimer's disease; HCHWA-D, hereditary cerebral hemorrhage with amyloidosis Dutch-type; $A\beta$ PP, amyloid β -protein precursor; tPA, tissue plasminogen activator; SDS-PAGE, sodium dodecyl sulfate polyacrylamide gel electrophoresis; CD, circular dichroism.

activation. Such a feedback mechanism could lead to excessive proteolysis in the vessel wall contributing to hemorrhagic stroke.

EXPERIMENTAL PROCEDURES

Materials. A β_{1-40} and A β_{6-40} peptides were synthesized by solid-phase Fmoc amino acid substitution, purified by reverse-phase HPLC and structurally characterized as previously described (21). Lyophilized A β peptides were initially resuspended in sterile distilled water to a concentration of 250 μ M (\approx 1 mg/mL) and then diluted to 0.1 mg/mL in the plasminogen activation assay described below. To prepare assembled forms of A β_{1-40} the peptide was resuspended to a final concentration of 2.5 mM in 50 mM Tris-HCl, 150 mM NaCl, pH 7.5, and incubated for 7 days at 37° C. An assembled β -sheet secondary structure was confirmed by circular dichroism spectroscopy and transmission electron microscopic analysis. Chemiluminescence reagents were from Amersham (Arlington Heights, IL). The chromogenic substrate Asp-Ala-Glu-Phe-Arg-*p*-nitroanilide (DAEFR-pNA) was synthesized by Multiple Peptide Systems (San Diego, CA). Tosyl-Gly-Pro-Lys-*p*-nitroanilide (Chromozym PL) was obtained from Boehringer-Mannheim (Indianapolis, IN). Glu-plasminogen (Glu-PLG), tPA, and plasmin were obtained from Calbiochem (La Jolla, CA).

Plasminogen Activation Assay. The conversion of plasminogen to plasmin by tPA in the absence or presence of unassembled or assembled A β_{1-40} was performed under first-order conditions with respect to plasminogen (15). Briefly, each reaction was performed in triplicate and contained 0.5 nM tPA and 0.5 μ M Glu-plasminogen in the absence or presence of the appropriate form of A β peptide at a concentration of 0.1 mg/mL. The reactions were performed in phosphate-buffered saline containing 0.01% Tween-80 and 0.1 mg/mL of bovine serum albumin in a final volume of 100–200 μ L. Each triplicate reaction was incubated at room temperature and at designated time points, 10 μ L aliquots were collected and added to 90 μ L of the above reaction buffer containing 0.5 mM Chromozym-PL in microtiter plate wells. The rate of plasmin cleavage of the chromogenic substrate was measured for 15 min at an absorbance of 405 nm in a kinetic microtiter plate reader (Molecular Devices). The obtained rates in mOD/min were converted to nM plasmin generated by comparison to established rates of chromogenic substrate hydrolysis by known amounts of purified plasmin. Experiments were independently repeated 3–4 \times .

Kinetic Parameters of Plasmin Cleavage of Chromogenic Substrates. The apparent K_m and V_{max} for plasmin cleavage of Chromozym-PL or DAEFR-pNA were obtained by measuring the rate of substrate hydrolysis (0.023–0.5 mM) by 10 nM plasmin. The mean \pm SD of each point performed in triplicate were analyzed by nonlinear least-squares fitting. The k_{cat} was determined by the ratio of the maximum rate of substrate hydrolysis (nM/s) divided by the concentration (nM) of plasmin. Experiments were independently confirmed 2 \times .

Proteolytic Processing of A β_{1-40} by Purified Plasmin. Soluble, unassembled A β_{1-40} at 0.1 mg/mL (\approx 25 μ M) was incubated alone or with purified plasmin (50 nM) or purified tPA (100 nM) for 6 h at 37° C in phosphate-buffered saline

containing 0.01% Tween-80. Aliquots of each reaction were electrophoresed on Tris/Tricine/SDS 10–20% gradient polyacrylamide gels and stained with Coomassie Brilliant Blue. In other experiments, aliquots of the reactions were electrophoresed on SDS 10% polyacrylamide gels, electroblotted onto nitrocellulose membranes, and subjected to chemiluminescence immunoblotting using an affinity purified rabbit anti-A β IgG (22) to visualize A β oligomers as previously described (21). The relative amounts of monomeric and oligomeric forms of A β were quantitated using a BioRad Fluor-S MultiImager System and the Multi-Analyst Image Analysis Software.

Amino Acid Sequence Analysis. A β_{1-40} (10 μ g) was incubated with 50 nM plasmin at 37° C for 6 h. An \approx 3.5 kDa plasmin-cleaved A β_{1-40} fragment was gel-purified by electrophoresis on a Tris/Tricine/SDS 10–20% polyacrylamide gel. The peptide was transferred to a poly(vinylidene difluoride) membrane and subjected to automated sequential Edman degradation analyses using a 475A protein sequencer.

Circular Dichroism Spectroscopy. Circular dichroism (CD) spectra were obtained using a JASCO J-715 spectropolarimeter. Aliquots of the freshly resuspended or assembled A β_{1-40} were diluted to a final concentration of 0.1 mg/mL in phosphate-buffered saline. The samples were loaded into a 0.1 cm quartz cell for measurements in the far-UV range of 190–250 nm. The instrument was calibrated using the standard ammonium D-10-camphor sulfonate in neodymium glass. Duplicate samples were scanned a minimum of 10 \times and final spectra were obtained after the subtraction of background readings of buffer only blanks. Analyses of the final spectra were performed using the Varselec method for determining secondary structure (23).

RESULTS

A β_{1-40} Stimulates Activation of Plasminogen by tPA. It was previously reported that assembled A β stimulated the activity of tPA in vitro (15). We investigated the stimulatory effect of A β on tPA activity using A β_{1-40} in both assembled and soluble form. Assembled A β_{1-40} was prepared as described in Experimental Procedures. CD spectral analysis showed that assembled A β_{1-40} possessed a strong β -pleated sheet structure, whereas freshly solubilized A β_{1-40} exhibited a random coil structure (Figure 1). TEM analysis confirmed the fibrillar nature of assembled A β_{1-40} (data not shown). Both the freshly solubilized and assembled A β_{1-40} were tested for their ability to stimulate the activation of plasminogen by tPA. As shown in Figure 2, in the absence of A β , there was minimal activation of plasminogen by tPA. On the other hand, in the presence of assembled A β_{1-40} , there was a striking increase in the rate of plasminogen activation. This was the result of a lower K_m and higher k_{cat} compared to unstimulated tPA (15). In the presence of freshly solubilized A β_{1-40} , there was a less robust increase in plasminogen activation during the initial 60 min of the reaction. However, after this time the rate of plasmin formation markedly increased approaching the rate obtained with the assembled A β_{1-40} . Assembled or freshly resuspended A β_{1-40} did not modulate the ability of plasmin to cleave its chromogenic substrate nor exhibited interactions with plasminogen or plasmin in solid-phase binding assays (data not shown). It is noteworthy that very similar results of an increased rate

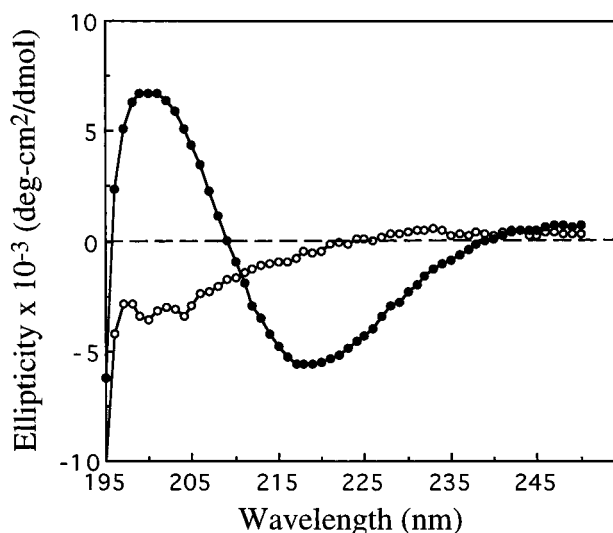


FIGURE 1: Secondary structural analysis of freshly solubilized and assembled preparations of $A\beta_{1-40}$ peptides. Freshly solubilized or assembled $A\beta_{1-40}$ was diluted to 0.1 mg/mL in phosphate-buffered saline and the secondary structure of each peptide preparation was determined by CD spectroscopy as described in Experimental Procedures. (○, freshly solubilized $A\beta_{1-40}$; ●, assembled $A\beta_{1-40}$.) Data represent means of 10 scans after the subtraction of background readings of buffer-only blanks.

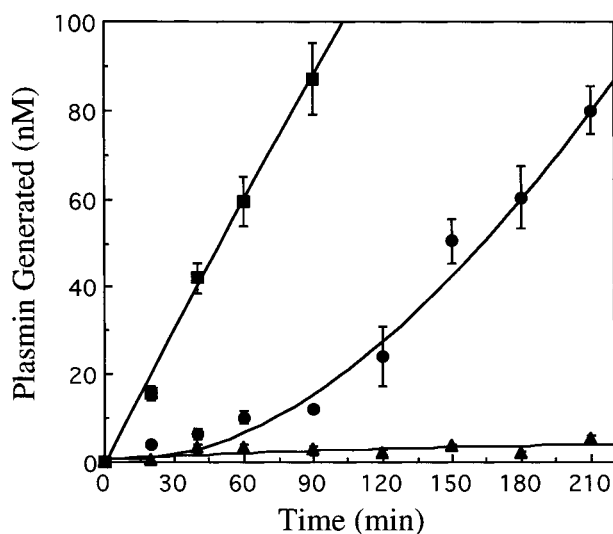


FIGURE 2: First-order activation of plasminogen by tPA in the absence or presence of freshly solubilized and assembled $A\beta_{1-40}$. Tissue PA (0.5 nM) and Glu-plasminogen (0.5 μ M) were incubated in the absence or presence of freshly solubilized or assembled $A\beta_{1-40}$ (0.1 mg/mL). At designated time points, aliquots were collected and the amount of plasmin generated was determined by measuring the hydrolysis of the substrate Chromozym-PL in a kinetic microtiter plate reader as described in Experimental Procedures. (▲, no $A\beta$; ●, freshly solubilized $A\beta_{1-40}$; ■, assembled $A\beta_{1-40}$.) The plotted results at each point represent the mean \pm S. D. of triplicate samples.

in plasmin formation over time were obtained in the plasminogen activation assay using freshly solubilized $A\beta_{1-40}$ containing the HCHWA-D mutation (data not shown).

Generation of Plasmin by tPA Leads to Cleavage of $A\beta$. The above finding with freshly solubilized $A\beta_{1-40}$ suggested that some component was changing in the plasminogen activation assay over time to further enhance the activity of tPA. Therefore, we decided to analyze the $A\beta$ in the reaction. Aliquots of the reaction mixture were collected at certain

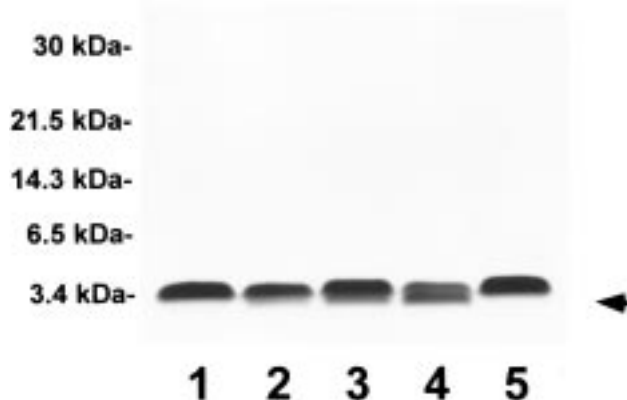


FIGURE 3: SDS-PAGE analysis of $A\beta_{1-40}$ in the plasminogen activation assay. Equal aliquots were collected from the plasminogen activation assay performed in the presence of freshly solubilized $A\beta_{1-40}$ and subjected to electrophoresis on Tris/Tricine/SDS 10–20% polyacrylamide gels followed by staining with Coomassie Brilliant Blue as described in Experimental Procedures. (Lane 1, zero timepoint; lane 2, 1 h timepoint; lane 3, 2 h timepoint; lane 4, 3 h timepoint; and lane 5, 3 h timepoint without tPA or plasminogen.) The arrow denotes ≈ 3.5 kDa truncated $A\beta$.

time points and subjected to SDS-PAGE on Tris/Tricine/SDS 10–20% polyacrylamide gels as described in Experimental Procedures. As shown in lane 1 of Figure 3, at the start of the reaction, only ≈ 4 kDa $A\beta_{1-40}$ is detected. After 1 h, a slight decrease in the ≈ 4 kDa $A\beta$ was noted accompanied by the appearance of a truncated ≈ 3.5 kDa $A\beta$ peptide (lane 2 in Figure 3). After 2 h and 3 h, the amount of ≈ 4 kDa $A\beta$ decreased even further and the amount of the truncated species continued to increase (lanes 3 and 4, respectively, in Figure 3). $A\beta_{1-40}$ incubated under identical conditions in the absence of tPA or plasminogen did not decrease nor form the ≈ 3.5 kDa species (lane 5 in Figure 3). These findings suggested that $A\beta_{1-40}$ was being proteolyzed during the course of the reaction.

Since both tPA and generated plasmin are present in the reaction mixture we determined which one was responsible for the observed cleavage of $A\beta_{1-40}$. The peptide was incubated with either purified tPA (100 nM) or plasmin (50 nM) and then analyzed by SDS-PAGE on a Tris/Tricine/SDS 10–20% polyacrylamide gel. As shown in lane 2 of Figure 4, when $A\beta_{1-40}$ was incubated with purified plasmin this resulted in a prominent truncated ≈ 3.5 kDa form of the peptide. On the other hand, $A\beta_{1-40}$ incubated with tPA did not result in cleavage of the peptide (lane 3 of Figure 4). It should be noted that the concentration of tPA used in this experiment was 200-fold higher than that used in the plasminogen activation experiments shown in Figures 2 and 3. These results indicated that it was the plasmin generated in the reaction that cleaved $A\beta$.

To identify the site of plasmin cleavage within $A\beta_{1-40}$, 10 μ g of the peptide was digested with 50 nM plasmin for 6 h. The resulting ≈ 3.5 kDa peptide was subjected to SDS-PAGE on a Tris/Tricine/SDS 10–20% polyacrylamide gel, electroblotted onto a poly(vinylidene difluoride) membrane, and subjected to amino terminal sequence analysis. The resulting sequence derived from five cycles of sequential Edman degradation is shown in Table 1. The amino terminal sequence of the truncated $A\beta$ peptide identified the plasmin cleavage site between Arg⁵-His⁶.

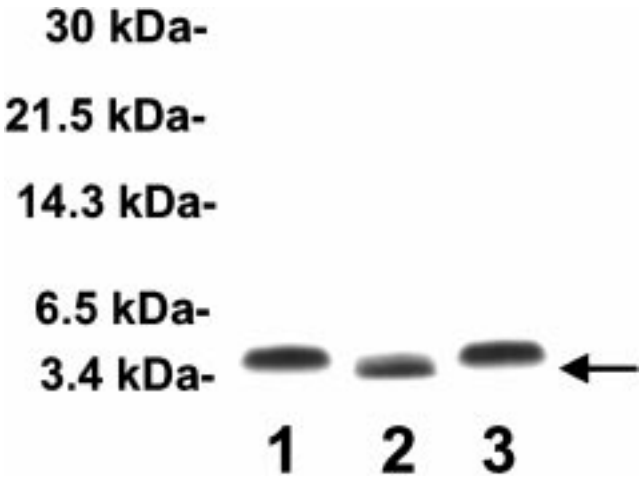


FIGURE 4: SDS-PAGE analysis of $A\beta_{1-40}$ incubated with purified plasmin or tPA. Freshly solubilized $A\beta_{1-40}$ (25 μ M) was incubated alone or in the presence of plasmin (50 nM) or tPA (100 nM) for 4 h. Aliquots were subjected to electrophoresis on Tris/Tricine/SDS 10–20% polyacrylamide gels and stained with Coomassie Brilliant Blue as described in Experimental Procedures. Lane 1, $A\beta_{1-40}$ alone; lane 2, $A\beta_{1-40}$ + plasmin; lane 3, $A\beta_{1-40}$ + tPA. The arrow denotes the \approx 3.5 kDa truncated $A\beta$ peptide derived from incubation with plasmin.

Table 1: Amino Acid Sequence Analysis of Plasmin Cleaved $A\beta_{1-40}$

residue	1	2	3	4	5	6	7	8	9	10
$A\beta$	D	A	E	F	R	H	D	S	G	Y
plasmin cleaved $A\beta^a$						H	D	S	G	Y

^a An \approx 3.5 kDa plasmin cleaved $A\beta_{1-40}$ fragment was prepared and subjected to five cycles of amino terminal amino acid sequence analysis as described under Experimental Procedures.

To further characterize plasmin cleavage of this $A\beta$ sequence we prepared a chromogenic substrate corresponding to the amino terminus of the peptide (DAEFR-pNA). The kinetics of cleavage of this $A\beta$ amino terminal sequence chromogenic substrate were compared to the commercially available chromogenic substrate for plasmin tosyl-Gly-Pro-Lys-pNA (Chromozym PL). As shown in Figure 5 and Table 2, DAEFR-pNA had slightly lower K_m and V_{max} values (91 μ M and 7.9 nM s^{-1} , respectively) compared to Chromozym-PL (107 μ M and 10.5 nM s^{-1} , respectively). This calculated to have a k_{cat} of 0.79 s^{-1} and 1.05 s^{-1} and a k_{cat}/K_m ratio of 0.0088 μ M $^{-1}$ s^{-1} and 0.0098 μ M $^{-1}$ s^{-1} for DAEFR-pNA and Chromozym-PL, respectively. Together, these findings indicate that the $A\beta$ amino terminal sequence is a comparably good chromogenic substrate for plasmin as Chromozym-PL, the commercially available chromogenic substrate for this enzyme.

Enhanced β -Sheet Secondary Structure and Stimulation of tPA by $A\beta_{6-40}$. The above studies clearly demonstrate that plasmin effectively cleaves between Arg⁵-His⁶ in $A\beta_{1-40}$ resulting, in the truncated $A\beta_{6-40}$ peptide. This truncated peptide was synthesized and purified to further characterize its structure and tPA stimulatory properties. Freshly resuspended $A\beta_{6-40}$ immediately adopted a strong β -sheet secondary structure in solution as determined by CD spectral analysis (Figure 6). This was in sharp contrast to $A\beta_{1-40}$, which assumed a random structure when freshly resuspended in solution (Figure 1). This is consistent with our previous findings showing that $A\beta_{1-40}$, under the concentrations used

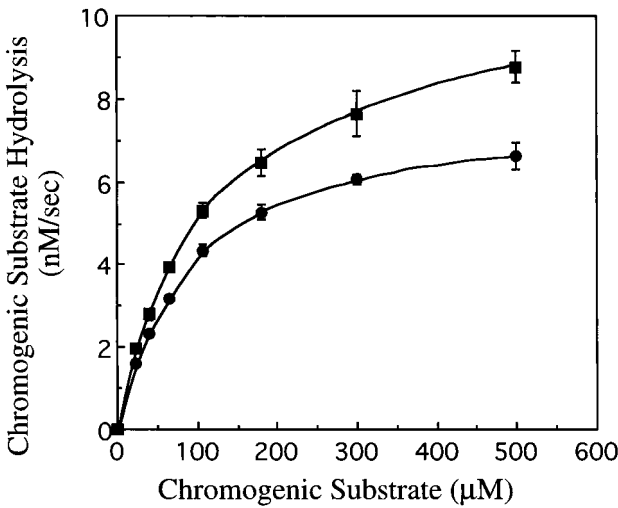


FIGURE 5: Plasmin hydrolysis of $A\beta$ amino terminal sequence chromogenic substrate. Substrate/velocity plot of plasmin hydrolysis of the $A\beta$ amino terminal sequence chromogenic substrate DAEFR-pNA (●) and the Chromozym-PL substrate (■). Initial rates of substrate hydrolysis were determined as described under Experimental Procedures. The plotted results at each point represent the mean \pm SD of triplicate determinations.

Table 2: Kinetic Analysis of Plasmin Cleavage of Chromogenic Substrates^a

substrate	K_m (μ M)	V_{max} (nM s^{-1})	k_{cat} (s^{-1})	k_{cat}/K_m (μ M $^{-1}$ s^{-1})
DAEFR-pNA ^b	91	7.9	0.79	0.0088
chromozym-PL ^c	107	10.5	1.05	0.0098

^a Human plasmin was used at a concentration of 10 nM. ^b $A\beta$ amino terminal sequence chromogenic substrate Asp-Ala-Glu-Phe-Arg-p-nitroanilide. ^c Tosyl-Gly-Pro-Lys-p-nitroanilide.

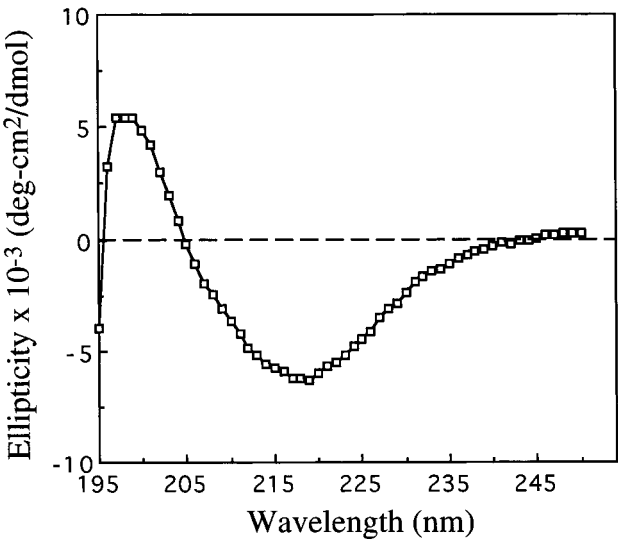


FIGURE 6: Secondary structural characterization of $A\beta_{6-40}$. $A\beta_{6-40}$ was freshly resuspended, diluted to 0.1 mg/mL in phosphate-buffered saline, and the secondary structure was determined by CD spectroscopy as described in Experimental Procedures. Data represent means of 10 scans after the subtraction of background readings of buffer-only blanks.

in our assays, maintains a random structure in solution when maintained for 6 days at 37 $^{\circ}$ C (24). To further demonstrate the structural differences between $A\beta_{1-40}$ and nascent $A\beta_{6-40}$ generated in our reactions, we performed SDS-PAGE analysis to visualize $A\beta$ oligomers as previously described

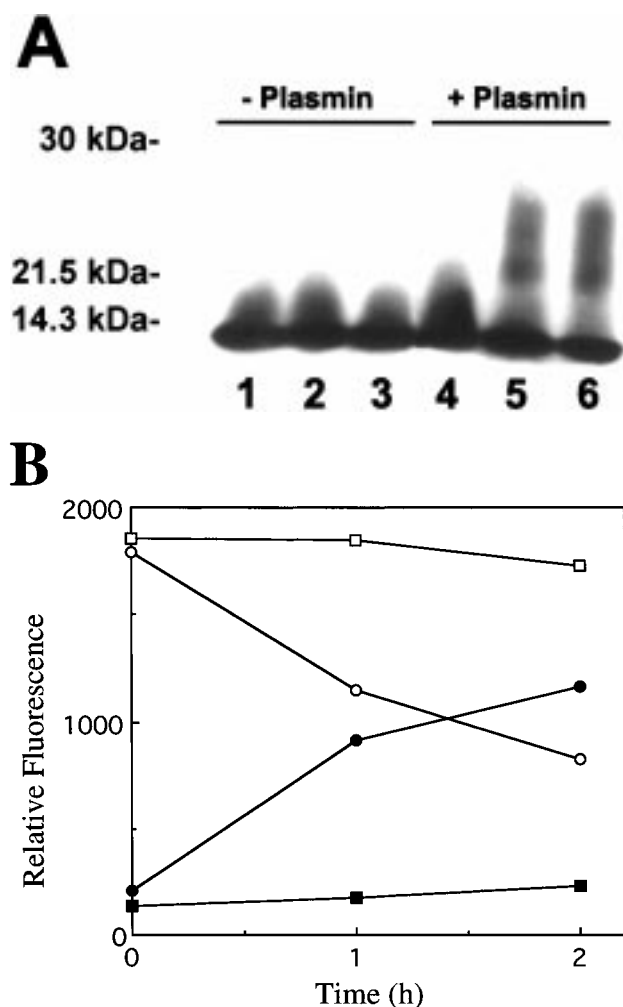


FIGURE 7: Plasmin-generated $A\beta_{6-40}$ forms SDS-stable oligomers. Freshly solubilized $A\beta_{1-40}$ ($25 \mu\text{M}$) was incubated alone or in the presence of 50 nM plasmin for increasing lengths of time. Aliquots were subjected to electrophoresis on SDS 10% polyacrylamide gels, electroblotted onto nitrocellulose membranes, and subjected to chemiluminescence immunoblotting using an affinity purified rabbit anti- $A\beta$ IgG as described in Experimental Procedures. (A) Lanes 1–3 are $A\beta_{1-40}$ alone and lanes 4–6 are $A\beta_{1-40}$ + plasmin. Lanes 1 and 4, zero timepoint; lanes 2 and 5, 1 h timepoint; lanes 3 and 6, 2 h timepoint. (B) The relative levels of monomeric and oligomeric $A\beta$ were quantitated from the immunoblot using a BioRad Fluor-S MultiImager. \square , monomeric $A\beta$ alone; \circ , monomeric $A\beta$ + plasmin; \blacksquare , oligomeric $A\beta$ alone; and \bullet , oligomeric $A\beta$ + plasmin.

by Burdick et al. (21). The cleavage of $A\beta_{1-40}$ by plasmin led to a decrease in monomeric $A\beta$ and a concomitant increase in SDS-stable $A\beta$ oligomers between 20 and 30 kDa (Figures 7A and 7B). In contrast, $A\beta_{1-40}$ incubated under similar conditions in the absence of plasmin failed to form these oligomeric structures (Figures 7A and 7B).

We next investigated the ability of $A\beta_{6-40}$ to stimulate the proteolytic activity of tPA in the plasminogen activation assay. Figure 8 shows that $A\beta_{6-40}$, with its strong β -sheet secondary structure, stimulates the activity of tPA to an extent that is comparable to the assembled form of $A\beta_{1-40}$. Together, these studies demonstrate that the amino terminal truncated $A\beta_{6-40}$ peptide, which results from plasmin cleavage of $A\beta_{1-40}$, exhibits enhanced β -sheet secondary structure, formation of stable oligomers, and tPA stimulatory properties.

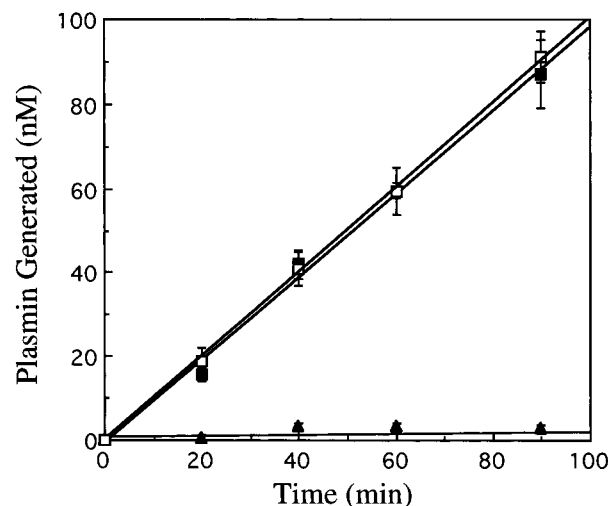


FIGURE 8: First-order activation of plasminogen by tPA in the absence or presence of fibrillar $A\beta_{1-40}$ and $A\beta_{6-40}$. Tissue PA (0.5 nM) and Glu-plasminogen ($0.5 \mu\text{M}$) were incubated in the absence or presence of assembled $A\beta_{1-40}$ or freshly resuspended $A\beta_{6-40}$ (0.1 mg/mL). At designated time points, aliquots were collected and the amount of plasmin generated was determined by measuring the hydrolysis of the substrate Chromozym-PL in a kinetic microtiter plate reader as described in Experimental Procedures. (\blacktriangle , no $A\beta$; \square , $A\beta_{6-40}$; \blacksquare , assembled $A\beta_{1-40}$.) The plotted results at each point represents the mean \pm SD of triplicate samples.

DISCUSSION

Although it is known that severe cerebrovascular $A\beta$ deposition can lead to hemorrhagic stroke the basis for this pathologic event has remained unclear. However, degeneration and loss of smooth muscle cells and their replacement with $A\beta$ fibrils in the cerebral vessel wall has been proposed to contribute to this devastating consequence. In this regard, studies have suggested a toxic response of smooth muscle cells to cerebrovascular $A\beta$ deposits in vivo (25–28). Moreover, recent cell culture studies indicate that certain forms of $A\beta$ can induce cell death and other pathologic responses in cerebrovascular smooth muscle cells (29–31). The $A\beta$ -induced degenerative responses appear to involve the assembly of the peptide into cell-surface fibrillar structures (24, 32).

In addition to the loss of smooth muscle cells, alterations in proteolytic mechanisms may also contribute to this process. For example, previous studies have shown that isoforms of $A\beta$ PP that contain the Kunitz-type proteinase inhibitor domain are potent inhibitors of several key enzymes of the coagulation cascade (33–36). In addition, both in vivo and in vitro studies have shown that cell types of the cerebral vessel wall exhibit increased expression of $A\beta$ PP in response to $A\beta$ deposition (24, 29–31, 37). Together, these findings have led to the postulate that increased expression of cerebrovascular $A\beta$ PP at sites of $A\beta$ deposition could lead to excessive inhibition of coagulation, thereby, contributing to hemorrhaging process (14, 34).

The present studies provide an additional dimension to the altered proteolytic mechanism hypothesis for hemorrhaging at sites of cerebrovascular $A\beta$ deposition. It was previously reported that assembled forms of $A\beta$ fragments stimulated tPA activation of plasminogen in vitro (15). Herein, we investigated the stimulation of tPA activation of plasminogen by freshly solubilized and assembled forms of

full-length $A\beta_{1-40}$. In these experiments, it was noted that the rate of tPA-mediated plasminogen activation dramatically increased over time using freshly solubilized $A\beta_{1-40}$ (Figure 2). This led to the novel finding that plasmin, the product of tPA mediated plasminogen activation, effectively cleaves $A\beta$ to yield a specific amino terminal truncated form of the peptide with altered secondary structure and enhanced tPA stimulatory properties. Such a feedback amplification mechanism involving cerebrovascular tPA and $A\beta$ could generate localized high levels of plasmin. It is noteworthy that tPA and plasminogen have been localized in the brain (38–40) and cerebral vasculature (41). Therefore, in the presence of a stimulator such as fibrillar $A\beta$ the necessary components are present that could initiate this proposed pathological cascade.

The cleavage of $A\beta$ by plasmin and the subsequent further stimulation of tPA could contribute to a hemorrhagic microenvironment in the cerebral vessel wall in several ways. For example, the cleavage of $A\beta$ by plasmin occurred between Arg⁵-His⁶ of the peptide. This site resides in the RHDS sequence of $A\beta$ reported to promote cell adhesion (42). Previously, we showed that coagulation factor XIa can also cleave this site in $A\beta$ and, thereby, abolish the cell adhesive properties of the peptide (43). This suggests that localized generation of plasmin could also disrupt this cell adhesive property of $A\beta$ and contribute to loss of cerebral vessel wall integrity. In addition, plasmin can either directly (44), or indirectly through proteolytic activation of a number of zymogens for matrix metalloproteinases (45, 46), proteolytically degrade extracellular matrix components. In this regard, several recent studies have implicated the involvement of tPA activation of plasminogen in neuronal cell death following induced excitotoxicity (47–49). The observed neuronal damage occurred in a fibrin-independent manner and likely involved degradation of matrix components (51, 52). In a similar manner, in cases of severe CAA excessive localized plasmin formation in the cerebral vasculature could significantly contribute to cell death and loss of vessel wall integrity resulting in a microenvironment that is conducive for hemorrhagic stroke.

REFERENCES

1. Vanley, C. T., Aguilar, M. J., Kleinhenz, R. J., and Lagios, M. D. (1981) *Hum. Pathol.* 12, 609–616.
2. Vinters, H. V. (1987) *Stroke* 18, 311–324.
3. Feldmann, E. (1991) *Stroke* 22, 684–691.
4. Mandybur, T. I. (1975) *Neurology* 25, 120–126.
5. Glenner, G. G., Henry, J. H., and Fujihara, S. (1981) *Ann. Pathol.* 1, 120–129.
6. van Duinen, S. G., Castano, E. M., Prelli, F., Bots, G. T. A. M., Luyendijk, W., and Frangione, B. (1987) *Proc. Natl. Acad. Sci. U.S.A.* 84, 5991–5994.
7. Luyendijk, W., Bots, G. T. A. M., Vegter-van der Vlisand Went, L. N. (1988) *J. Neurool. Sci.* 85, 267–280.
8. Wattendorff, A. R., Frangione, B., Luyendijk, W., and Bots, G. T. A. M. (1995) *J. Neurol. Neurosurg. Psychiatry* 59, 699–705.
9. Glenner, G. G. and Wong, C. W. (1984) *Biochem. Biophys. Res. Commun.* 122, 885–890.
10. Prelli, F., Castano, E., Glenner, G. G., and Frangione, B. (1988) *J. Neurochem.* 51, 648–651.
11. Selkoe, D. J. (1996) *J. Biol. Chem.* 271, 18295–18298.
12. Yankner, B. A. (1996) *Neuron* 16, 921–932.
13. Masters, C. L., Simms, G., Weinman, N. A., Multhaup, G., McDonald, B. L., and Beyreuther, K. (1985) *Proc. Natl. Acad. Sci. U.S.A.* 82, 4245–4269.
14. Van Nostrand, W. E., Schmaier, A. H., and Wagner, S. L. (1992) *Ann. N. Y. Acad. Sci.* 674, 243–252.
15. Kingston, I. B., Castro, M. J. M., and Anderson, S. A. (1995) *Nature Med.* 1, 138142.
16. Okazaki, H., Reagen, T. J., and Campbell, R. J. (1979) *Mayo Clin. Proc.* 54, 22–31.
17. Maruyama, K., Ikeda, S., Ishihara, T., Allsop, D., and Yanagisawa, N. (1990) *Stroke* 21, 397–403.
18. Stern, R. A., Trojanowski, J. A., and Lee, V. M.-L. (1990) *FEBS Lett.* 264, 43–47.
19. Pendlebury, W. W., Iole, E. D., Tracy, R. P., and Dill, B. A. (1989) *Ann. Neurol.* 29, 210–213.
20. Wijicks, E. F. M., and Jack, C. R. (1993) *Stroke* 24, 554–557.
21. Burdick, D., Soreghan, B., Kwon, M., Kosmoski, J., Knauer, M., Henschen, A., Yates, J., Cotman, C., and Glabe, C. (1992) *J. Biol. Chem.* 267, 546–554.
22. Davis-Salinas, J., Saporito-Irwin, S. M., Donovan, F. M., Cunningham, D. D., and Van Nostrand, W. E. (1994) *J. Biol. Chem.* 269, 22623–22627.
23. Johnson, W. C., Jr. (1988) *Annu. Rev. Biophys. Chem.* 17, 145–166.
24. Van Nostrand, W. E., Melchor, J. P., and Ruffini, L. (1998) *J. Neurochem.* 70, 216–223.
25. Coria, F., Larrondo-Lillo, M., and Frangione, B. (1989) *J. Neuropathol. Exp. Neurol.* 48, 368–375.
26. Kawai, M., Kalaria, R. N., Cras, P., Siedlak, S. L., Velasco, M. E., Shelton, E. R., Chan, H. W., Greenberg, B. D., and Perry, G. (1993) *Brain Res.* 623, 142–146.
27. Wisniewski, H. M., Frackowiak, J., Zoltowska, A., and Kim, K. S. (1994) *Amyloid* 1, 8–16.
28. Wisniewski, H. M. and Weigel, J. (1994) *Acta Neuropathol.* 87, 233–241.
29. Davis-Salinas, J., Saporito-Irwin, S. M., Cotman, C. W., and Van Nostrand, W. E. (1995) *J. Neurochem.* 65, 931–934 (1995).
30. Davis-Salinas, J., and Van Nostrand, W. E. (1995) *J. Biol. Chem.* 270, 20887–20890.
31. Davis, J., and Van Nostrand, W. E. (1996) *Proc. Natl. Acad. Sci. U.S.A.* 93, 2996–3000.
32. Verbeek, M. M., de Waal, R. M. W., Schipper, J. J., and Van Nostrand, W. E. (1997) *J. Neurochem.* 68, 1135–1141.
33. Van Nostrand, W. E., Wagner, S. L., Farrow, J. S., and Cunningham, D. D. (1990) *J. Biol. Chem.* 265, 9591–9594.
34. Schmaier, A. H., Dahl, L. D., Rozemuller, A. J. M., Roos, R. A. C., Wagner, S. L., Chung, R., and Van Nostrand, W. E. (1993) *J. Clin. Invest.* 92, 2540–2545.
35. Schmaier, A. H., Dahl, L. D., Hasan, A. A. K., Cines, D. B., and Van Nostrand, W. E. (1995) *Biochemistry* 34, 1171–1178.
36. Mahdi, F., Van Nostrand, W. E., and Schmaier, A. H. (1995) *J. Biol. Chem.* 270, 23468–23474.
37. Rozemuller, A. J. M., Roos, R. A. C., Bots, G. T. A. M., Kamphorst, W., Eikelenboom, P., and Van Nostrand, W. E. (1993) *Am. J. Pathol.* 142, 1449–1457.
38. Sappino, A., Madani, R., Huarte, J., Belin, D., Kiss, J., Wohlwend, A., and Vassalli, J.-D. (1993) *J. Clin. Invest.* 92, 679–685.
39. Rickles, R., and Strickland, S. (1988) *FEBS Lett.* 229, 100–106.
40. Carroll, P., Tsirka, S., Richards, W., Frohman, M., and Strickland, S. (1994) *Development* 120, 3173–3183.
41. Schreiber, S. S., Tan, Z., Sun, N., Wang, L., and Zlokovic, B. V. (1998) *Neurosurg.* 43, 909–913.
42. Ghiso, J., Rostagno, A., Gardella, J. E., Liem, L., Gorevic, P. D., and Frangione, B. (1992) *Biochem. J.* 288, 1053–1059.

43. Saporito-Irwin, S. M., and Van Nostrand, W. E. (1995) *J. Biol. Chem.* 270, 26265–26269.
44. Mignatti, P., and Rifkin, D. B. (1993) *Physiol. Rev.* 73, 161–195.
45. Okumura, Y., Sato, H., Seiki, M., and Kido, H. (1997) *FEBS Lett.* 402, 181–184.
46. Mazzieri, R., Masiero, L., Zanetta, L., Monea, S., Onisto, M., Garbisa, S., and Mignatti, P. (1997) *EMBO J.* 16, 2319–2332.
47. Tsirka, S. E., Gualandris, A., Amaral, D. G., and Strickland, S. (1995) *Nature* 377, 340–344.
48. Tsirka, S. E. (1997) *J. Mol. Med.* 75, 341–347.
49. Wang, Y. F., Tsirka, S. E., Strickland, S., Stieg, P. E., Soriano, S. G., and Lipton, S. A. (1998) *Nature Med.* 4, 228–231.
50. Tsirka, S. E., Bugge, T. H., Degen, J. L., and Strickland, S. (1997) *Proc. Natl. Acad. Sci. U.S.A.* 94, 9779–9781.
51. Tsirka, S. E., Rogove, A. D., Bugge, T. H., Degen, J. L., and Strickland, S. (1997) *J. Neurosci.* 17, 543–552.

BI990610F